

Optimization of LED illumination for generating metamerism
Daisuke Miyazaki, Mia Nakamura, Masashi Baba, Ryo Furukawa, Shinsaku Hiura,
Journal of Imaging Science and Technology,
vol. 60, no. 6, pp. 60502-1-60502-15, 2016.11

This file is a draft version. It may be different from the published version.

Optimization of LED Illumination for Generating Metamerism

Daisuke Miyazaki,^{1, a)} Mia Nakamura,^{1, b)} Masashi Baba,¹ Ryo Furukawa,¹ and Shinsaku Hiura¹
Hiroshima City University, Graduate School of Information Sciences, 3-4-1 Ozukahigashi, Asaminami-ku, Hiroshima City, 731-3194, Japan

Metamerism is the phenomenon by which two objects are recognized as having different colors under one light source and the same color under another light source. In this article, the authors propose a method for creating trick artwork using metamerism. Two illuminants are designed to achieve metamerism such that two oil paints used in a piece of artwork look the same under one light but different under another light. The experimental results show that metamerism is generated between the two light sources and the two object colors.

I. INTRODUCTION

The phenomenon by which two objects are recognized as having different colors under one light source but as the same color under another light source is called metamerism. Metamerism, which can cause the colors of clothing and printed materials to vary under fluorescent lighting and sunlight, is known as a source of annoyance among designers and photographers, as well as those in the apparel, printing, and advertising industries. This article rebels against such common sense and fully brings out the value of metamerism, which has been disregarded in the past. The proposed method involves a multispectrum database of many types of light-emitting diode (LED). Two sets of light sources have been designed as mixtures of these LEDs so that two certain kinds of oil paint look identical under one but different under the other.

II. RELATED WORK

Computer-aided art software has made it possible for users to create artwork that would have been very difficult to create manually¹⁻⁸. This article proposes a new computer-aided art system. Our system can be used to create metameric art such as that presented by Valluzzi⁹. Unlike Valluzzi⁹, whose purpose was not to express intended figures, the objective of this paper is to design an illumination that can achieve metamerism so as to represent premeditated shapes.

Bala et al.¹⁰ also made watermarks using metamerism; because CMYK printers can express black-colored prints either with key (K) ink or cyan, magenta, and yellow (CMY) inks, they printed one of their black colors using K ink and another black color using CMY ink. These colors appear the same under natural light but different when illuminated by LEDs of certain wavelengths. They selected an LED with a peak wavelength at which the spectral energies of two inks are sufficiently far apart to be distinguished visually. Drew and Bala¹¹ improved their method to exaggerate the color difference¹⁰. Unlike Bala et al.^{10,11}, we have designed an illumination that creates metamerism with user-suggested paints by combining different types of LEDs.

Finlayson et al.^{12,13} proposed a calculation method for a spectral distribution that achieves metamerism; their method produces various sets of spectral distributions that appear to have the same color as a given RGB or XYZ value. Although, in theory, an infinite number of spectral distributions appear to be the same color, Finlayson et al. confined the scope of their article to those that could be expressed as linear sums of the spectral distributions of the Macbeth (X-rite) color checker. In our article, we use LED spectral distributions as our database instead of Macbeth color checker distributions, since we aim to design the illuminants using our LED database.

Miyazaki et al.¹⁴⁻¹⁶ proposed a method for calculating the blending ratios of paint that generate the metamerism in response to light sources suggested by the user. The paints have wide-band spectral distributions, whereas the LEDs have narrow-band spectral distributions, which can better represent custom-built spectral distributions by using different LED combinations. Kobayashi et al.¹⁷ proposed a method for detecting cultivation colonies using images obtained by illuminating the medium with LEDs of different wavelengths. Unlike Miyazaki et al.¹⁴⁻¹⁶, who used paints for metameric art, Kobayashi¹⁷ and Bala¹⁰ have shown that LEDs are useful for enhancing color differences; their methods use only one LED for illuminating a single scene. This article proposes a method that calculates the LED-mixing ratios that generate the most metamerism possible given the oil paints used. We then create pieces of artwork that take advantage of the metamerism occurring between the two suggested object colors under the two designed illuminant colors.

III. PERCEPTION OF REFLECTED LIGHT

The XYZ color system^{18,19} is a representative method for expressing human perceptions of colors and was defined by the Commission Internationale de l'Eclairage. It can express the colors perceived by the human brain stimulated by photoreceptor cells. The X, Y, and Z correspond to red, green, and blue, respectively. In general, the lower limit wavelength of visible light is approximately 380–420 nm, and the upper limit is approximately 680–800 nm²⁰⁻²³. In this article, we consider light with wavelengths varying from 400 to 800 nm because our measurement device can only measure spectral distributions within this range. Expressing the color-matching functions of X, Y, and Z for a wavelength λ as $\bar{x}(\lambda)$, $\bar{y}(\lambda)$, and $\bar{z}(\lambda)$, respectively, the observed X, Y, and Z values are

^{a)}miyazaki@hiroshima-cu.ac.jp

^{b)}Presently with FUJITSU Kansai-Chubu Net-Tech, Ltd.

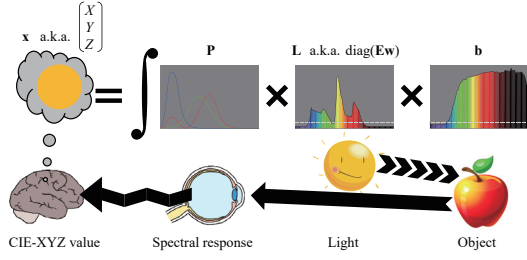


FIG. 1. The mechanism of perception of visible light.

expressed as follows (Figure 1):

$$X = \int_{400}^{800} L(\lambda)B(\lambda)\bar{x}(\lambda)d\lambda, \quad (1)$$

$$Y = \int_{400}^{800} L(\lambda)B(\lambda)\bar{y}(\lambda)d\lambda, \quad (2)$$

$$Z = \int_{400}^{800} L(\lambda)B(\lambda)\bar{z}(\lambda)d\lambda. \quad (3)$$

Here, $L(\lambda)$ is the spectral distribution of the light source and $B(\lambda)$ is the spectral reflectance of the object surface. The above equations express the spectral distributions as continuous functions, but the observed spectral distributions are discrete. In this article, wavelengths ranging from 400 to 800 nm are discretized with constant intervals of $(800 - 400)/N_b$, where N_b is the number of bands used to discretize the spectral range. Expressing the observed values as $\mathbf{x} = (X, Y, Z)^T$, Eqs. (1)–(3) can be expressed as follows:

$$\mathbf{x} = \mathbf{P}\mathbf{L}\mathbf{b}. \quad (4)$$

We express the discretized data of the color-matching functions as the $3 \times N_b$ matrix \mathbf{P} , and place the X, Y, and Z color-matching functions in each row:

$$\mathbf{P} = \begin{pmatrix} \bar{x}_1 & \bar{x}_2 & \cdots & \bar{x}_{N_b} \\ \bar{y}_1 & \bar{y}_2 & \cdots & \bar{y}_{N_b} \\ \bar{z}_1 & \bar{z}_2 & \cdots & \bar{z}_{N_b} \end{pmatrix}. \quad (5)$$

We express the observed spectral distribution as an $N_b \times 1$ vector \mathbf{b} . The spectrum of the illumination source $\mathbf{l} = (l_1, l_2, \dots, l_{N_b})^T$ is expressed by an $N_b \times N_b$ diagonal matrix, \mathbf{L} :

$$\mathbf{L} = \text{diag}(\mathbf{l}) = \begin{pmatrix} l_1 & 0 & \cdots & 0 \\ 0 & l_2 & \cdots & 0 \\ \vdots & \vdots & \ddots & \vdots \\ 0 & 0 & \cdots & l_{N_b} \end{pmatrix}. \quad (6)$$

In this article, “diag” represents a function that aligns each element of the vector onto the diagonal elements of a matrix to form a diagonal matrix.

IV. LIGHT-MIXING MODEL

Our purpose is to create artwork by mixing LEDs. In this section, we explain the mathematical model used to calculate

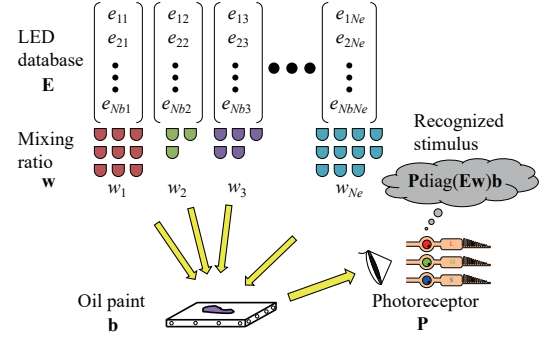


FIG. 2. Illumination design using an LED database.

the mixed illumination.

We express the spectral reflectance of N_e types of LEDs as an $N_b \times N_e$ matrix, \mathbf{E} :

$$\mathbf{E} = \begin{pmatrix} e_{11} & e_{12} & \cdots & e_{1N_e} \\ e_{21} & e_{22} & \cdots & e_{2N_e} \\ \vdots & \vdots & \ddots & \vdots \\ e_{N_b1} & e_{N_b2} & \cdots & e_{N_bN_e} \end{pmatrix}. \quad (7)$$

We make mixed-light illumination by combining N_e LEDs with N_e mixing ratios. We express the mixing ratios using an $N_e \times 1$ vector \mathbf{w} (Fig. 2).

The mixed light can be calculated by a linear summation model^{12,13,24}:

$$\mathbf{L} = \text{diag}(\mathbf{E}\mathbf{w}). \quad (8)$$

Each element of the vector $\mathbf{l} = \mathbf{E}\mathbf{w}$ is described as follows.

$$\begin{aligned} l_1 &= w_1e_{11} + w_2e_{12} + \cdots + w_{N_e}e_{1N_e}, \\ l_2 &= w_1e_{21} + w_2e_{22} + \cdots + w_{N_e}e_{2N_e}, \\ &\vdots \\ l_{N_b} &= w_1e_{N_b1} + w_2e_{N_b2} + \cdots + w_{N_e}e_{N_bN_e}. \end{aligned}$$

This model is well known as an additive color mixture model²⁴. Finlayson et al.^{12,13} also used this model for the analysis of metamerism.

Let us now explain a specific example of Eq. (8). Figure 3 shows an example of 10 LED bulbs. Let 10 times the spectral radiance of light source 1 be e_1 and 10 times that of light source 2 be e_2 . Fig. 3 (a) illustrates 10 bulbs of light source 1; thus, its spectral radiance is e_1 . Fig. 3 (b) illustrates 10 bulbs of light source 2; thus, its spectral radiance is e_2 . Fig. 3 (c) shows an arrangement of 7 bulbs of light source 1 and 3 bulbs of light source 2; thus, the spectral radiance is $\frac{7}{10}e_1 + \frac{3}{10}e_2$. In this example, we multiplied the radiance by 10 for simplicity, as there are 10 LED bulbs for this specific example (Fig. 3). There is no other purpose behind the specific value of “10” used in our method. Because scaling the brightness of light by 10 or any other value does not affect the subsequent computation, we do not multiply the actual database \mathbf{E} by 10 or by any other value as it is unnecessary.

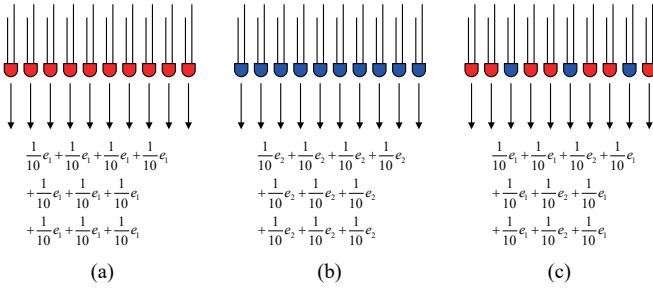


FIG. 3. Linear summation of multiple LEDs.

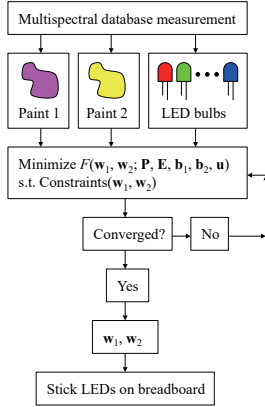


FIG. 4. Schematic flow of our proposed method.

V. PROPOSED METHOD

In this section, we explain the proposed method for automatically calculating the mixing ratios for LEDs to generate metamerism. Two paints are referred to as paint 1 and paint 2. We also represent two types of mixed illumination as mixed source 1 and mixed source 2. We calculate the mixing ratios such that paints 1 and 2 have the same color and brightness under mixed source 1, but appear to have different colors or brightnesses under mixed source 2. Our algorithm constrains both the color of mixed source 1 and the color of mixed source 2 to be the same. This is because we want the two illuminants to be perceived as having the same color by the human eyes but to be different in the spectral domain. Our aim is to create a trick artwork whereby two paints look different under a certain colored light but the same under another light of the same color. If the user decides to illuminate their artwork using an illuminant of a specific color, our algorithm can constrain the illuminant color to be as similar as possible to the user-specified color. A flowchart of our method is shown in Figure 4. We first measure the spectral distributions of the paints and the LEDs (Experimental Setup section). Next, we calculate the mixing ratios for the LEDs (this section). Finally, we illuminate the paints using the designed source (Experimental Results section).

A schematic explanation of our algorithm is shown in Figure 5, and the detailed explanation is as follows. We denote

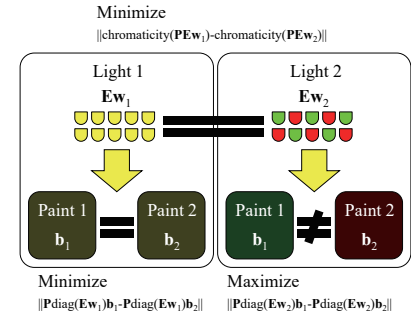


FIG. 5. The metamerism generated when two paints are illuminated by two different lights.

the spectral distribution of paint 1 as \mathbf{b}_1 and that of paint 2 as \mathbf{b}_2 . The mixing ratio of the LEDs to make mixed source 1 is denoted as \mathbf{w}_1 and that to make mixed source 2 is denoted as \mathbf{w}_2 . Therefore, the spectral distributions of mixed sources 1 and 2 can be represented as $\mathbf{E}\mathbf{w}_1$ and $\mathbf{E}\mathbf{w}_2$, respectively, in vector representation, and as $\text{diag}(\mathbf{E}\mathbf{w}_1)$ and $\text{diag}(\mathbf{E}\mathbf{w}_2)$ in matrix representation.

The spectral distribution of paint 1, illuminated by mixed source 1, can be calculated as $\text{diag}(\mathbf{E}\mathbf{w}_1)\mathbf{b}_1$, and the perceived color will be $(X_{11}, Y_{11}, Z_{11})^\top = \mathbf{P}\text{diag}(\mathbf{E}\mathbf{w}_1)\mathbf{b}_1$. The spectral distribution of paint 2, illuminated by mixed source 1, can be calculated as $\text{diag}(\mathbf{E}\mathbf{w}_1)\mathbf{b}_2$, and the perceived color will be $(X_{12}, Y_{12}, Z_{12})^\top = \mathbf{P}\text{diag}(\mathbf{E}\mathbf{w}_1)\mathbf{b}_2$. We minimize the difference between these two colors, i.e., we minimize $\|(X_{11}, Y_{11}, Z_{11})^\top - (X_{12}, Y_{12}, Z_{12})^\top\|$. More specifically, we minimize the following metric.

$$\sqrt{(X_{11} - X_{12})^2 + (Y_{11} - Y_{12})^2 + (Z_{11} - Z_{12})^2}. \quad (9)$$

The spectral distribution of paint 1, illuminated by mixed source 2, can be calculated as $\text{diag}(\mathbf{E}\mathbf{w}_2)\mathbf{b}_1$, and the perceived color will be $(X_{21}, Y_{21}, Z_{21})^\top = \mathbf{P}\text{diag}(\mathbf{E}\mathbf{w}_2)\mathbf{b}_1$. The spectral distribution of paint 2, illuminated by mixed source 2, can be calculated as $\text{diag}(\mathbf{E}\mathbf{w}_2)\mathbf{b}_2$, and the perceived color will be $(X_{22}, Y_{22}, Z_{22})^\top = \mathbf{P}\text{diag}(\mathbf{E}\mathbf{w}_2)\mathbf{b}_2$. We maximize the difference between these two colors, i.e., we maximize $\|(X_{21}, Y_{21}, Z_{21})^\top - (X_{22}, Y_{22}, Z_{22})^\top\|$. More specifically, we maximize the following metric.

$$\sqrt{(X_{21} - X_{22})^2 + (Y_{21} - Y_{22})^2 + (Z_{21} - Z_{22})^2}. \quad (10)$$

The chromaticity of mixed source 1 is represented as $(x_1, y_1)^\top = f(\mathbf{P}\mathbf{E}\mathbf{w}_1)$ and the chromaticity of mixed source 2 is represented as $(x_2, y_2)^\top = f(\mathbf{P}\mathbf{E}\mathbf{w}_2)$. Function $f : (X, Y, Z) \rightarrow (x, y)$ converts XYZ to xy-chromaticity^{18,19}:

$$f \begin{pmatrix} X \\ Y \\ Z \end{pmatrix} = \begin{pmatrix} x \\ y \end{pmatrix} = \begin{pmatrix} \frac{X}{X + Y + Z} \\ \frac{Y}{X + Y + Z} \end{pmatrix}. \quad (11)$$

As usual, the chromaticity $z = Z/(X + Y + Z)$ is not used to avoid redundancy because $x + y + z = 1$ holds. To make the

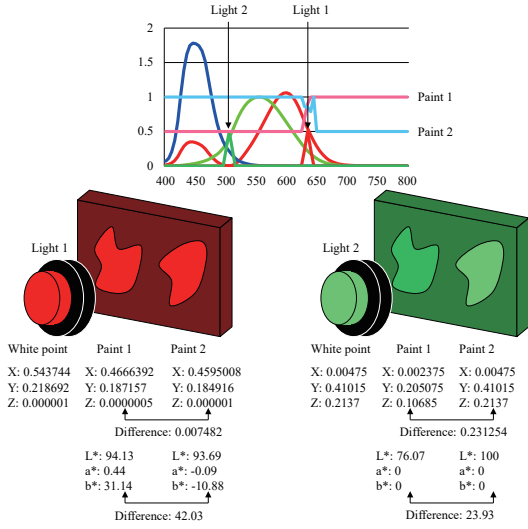


FIG. 6. Evaluating CIE-XYZ rather than CIE-L*a*b* for the cost function results in a stable computation.

colors of mixed source 1 and mixed source 2 as similar as possible, we minimize the difference between the chromaticities. Thus, we minimize $\|(x_1, y_1)^\top - (x_2, y_2)^\top\|$. More specifically, we minimize the following metric:

$$\sqrt{(x_1 - x_2)^2 + (y_1 - y_2)^2}. \quad (12)$$

We use xy -chromaticity in this article, but our plan in the future is to use the a^*b^* chromaticity of $L^*a^*b^*$ color space, which is closer to human perception. It should be noted that we evaluate the difference between the XYZ values instead of the $L^*a^*b^*$ values for calculating the color difference under mixed source 1 (Eq. (9)) and that under mixed source 2 (Eq. (10)). Because LEDs have a narrow-band spectral distribution, there is a problem, shown in Figure 6, in stably calculating the $L^*a^*b^*$ values. The human eye has color constancy, which allows recognition of a white object under colored light. To cancel the color of the light, the $L^*a^*b^*$ color system first divides the XYZ values of the target object by that of the white point. Therefore, the $L^*a^*b^*$ values will be unstable because the XYZ values become 0 or close to 0 for a certain light. The installation of $L^*a^*b^*$ color space in our algorithm needs further investigation to work stably with our software.

Specification of the color of illuminants is convenient for artists who wish to design their own metameric artwork. Suppose that the user has specified a certain chromaticity $\mathbf{u} = (x_u, y_u)^\top$. If we minimize the difference between the chromaticity of the user-specified value and the mixed sources ($(x_1, y_1)^\top$ and $(x_2, y_2)^\top$), the user can obtain mixed sources with the user-specified color. We minimize one of the following metrics, depending on which has the largest value.

$$\sqrt{(x_1 - x_u)^2 + (y_1 - y_u)^2}, \quad (13)$$

$$\sqrt{(x_2 - x_u)^2 + (y_2 - y_u)^2}.$$

To summarize, the cost function $F(\cdot)$ that must be minimized to realize the intended appearance is as follows:

$$\{\mathbf{w}_1, \mathbf{w}_2\} = \underset{\mathbf{w}_1, \mathbf{w}_2}{\operatorname{argmin}} F(\mathbf{w}_1, \mathbf{w}_2; \mathbf{P}, \mathbf{E}, \mathbf{b}_1, \mathbf{b}_2, \mathbf{u}), \quad (14)$$

$$F(\mathbf{w}_1, \mathbf{w}_2; \mathbf{P}, \mathbf{E}, \mathbf{b}_1, \mathbf{b}_2, \mathbf{u}) =$$

$$a_1 \|\mathbf{P} \operatorname{diag}(\mathbf{E} \mathbf{w}_1) \mathbf{b}_1 - \mathbf{P} \operatorname{diag}(\mathbf{E} \mathbf{w}_1) \mathbf{b}_2\|^2$$

$$- a_2 \|\mathbf{P} \operatorname{diag}(\mathbf{E} \mathbf{w}_2) \mathbf{b}_1 - \mathbf{P} \operatorname{diag}(\mathbf{E} \mathbf{w}_2) \mathbf{b}_2\|^{0.5}$$

$$+ a_3 \|f(\mathbf{P} \mathbf{E} \mathbf{w}_1) - f(\mathbf{P} \mathbf{E} \mathbf{w}_2)\|^2$$

$$+ a_4 \max\{\|f(\mathbf{P} \mathbf{E} \mathbf{w}_1) - \mathbf{u}\|^2, \|f(\mathbf{P} \mathbf{E} \mathbf{w}_2) - \mathbf{u}\|^2\}, \quad (15)$$

where

$$\sum_{n=1}^{N_e} w_{1n} = 1, \quad \sum_{n=1}^{N_e} w_{2n} = 1, \quad (16)$$

$$\sum_{n=1}^{N_e} w_{1n} N_l = N_l, \quad \sum_{n=1}^{N_e} w_{2n} N_l = N_l. \quad (17)$$

Moreover, for $n = 1, \dots, N_e$,

$$w_{1n} \geq 0, \quad w_{2n} \geq 0, \quad (18)$$

$$w_{1n} N_l = \lfloor w_{1n} N_l \rfloor, \quad w_{2n} N_l = \lfloor w_{2n} N_l \rfloor, \quad (19)$$

where a_1, a_2, a_3 , and a_4 in Eq. (15) are non-negative constants, which we explain later. The reason why the first term of Eq. (15) is raised to the power of 2 and the second term to the power of 0.5 is explained later in this section. Equations (17) and (19) are also explained later in this section. Although we have already outlined the sizes of each mathematical variable, we again summarize this information here for the readers' convenience: \mathbf{P} is a $3 \times N_b$ matrix, \mathbf{E} is an $N_b \times N_e$ matrix, \mathbf{w}_1 and \mathbf{w}_2 are N_e -dimensional column vectors, \mathbf{b}_1 and \mathbf{b}_2 are N_b -dimensional column vectors, and \mathbf{u} is a 2-dimensional column vector.

The constants a_1, a_2, a_3 , and a_4 are set manually. If we were to use a small value for a_1 , the first term of Eq. (15) would not become sufficiently small, so paint 1 and paint 2 under mixed source 1 would not be similar enough. On the other hand, if we set a large value for a_1 , paint 1 and paint 2 under mixed source 1 become closer, but other conditions are more difficult to satisfy. For example, paint 1 and paint 2 under mixed source 2 would not be sufficiently different because the relative value of a_2 compared with a_1 would be very small. Therefore, depending on the database, we set the best balance between these constant values to obtain better results. If we set a_3 to be 0, the chromaticities of mixed source 1 and mixed source 2 would not be the same. The larger the value of a_3 is, the closer the chromaticities of mixed source 1 and mixed source 2 are. If the chromaticities of the mixed sources are not specified by the user, as is shown in Fig. 5, we set $a_4 = 0$, whereas if the user specifies them, as is shown in the Colors Specified by the User section, we set $a_4 > 0$.

In Eq. (15), we took the square of the first term to increase its weight and the square root of the second term to reduce its weight. The preliminary experiment empirically confirmed that setting these weights allows stable determination of a solution¹⁵. As is described in the literature¹⁵, these weights are set because human eyes tend to exaggerate slight differences in color and brightness. Since the weight of the first

term is larger than that of the second term, our software tries to minimize the first term much more than the second term. Thus, the slight color difference represented by the first term is suppressed. Finding spectral distributions that become the same color is difficult. On the other hand, an infinite variety of spectral distributions that can express different colors exist. Thus, this is another reason for setting such weights.

Because Eq. (14) is a complicated function with multiple constraints, we employ a simulated annealing method²⁵ based on the Nelder–Mead downhill simplex method²⁵ to solve it stably. The first and second terms of Eq. (15) consider not only the chromaticity but also the brightness because the resultant illuminants must satisfy the requirement of enabling artistic illusion. When observing a scene illuminated only by mixed source 1 and another scene illuminated only by mixed source 2, human pupils and photoreceptors automatically adjust for the brightness; thus, the difference in brightness between mixed source 1 and mixed source 2 does not affect our method. However, the brightness calculated for mixed source 1 and that for mixed source 2 must be simultaneously evaluated using Eq. (15). Thus, the sum of the elements of $\mathbf{E}\mathbf{w}_1$ is set to 1. Further, the sum of the elements of $\mathbf{E}\mathbf{w}_2$ is set to 1. Any normalization procedures can be employed since the normalization does not affect human perception because of its ability to automatically adjust to incoming light. Equation (15) can be stably solved by adequately adjusting the coefficients a_1 and a_2 , regardless of the normalization procedure used.

The Nelder–Mead downhill simplex method²⁵ expresses the parameters to be solved as a simplex with $2N_e + 1$ apexes represented in a $2N_e$ -dimensional solution space. This simplex moves like an amoeba in the solution space toward the final solution where the value of the cost function is small.

The parameters \mathbf{w}_1 and \mathbf{w}_2 are normalized when evaluating the cost function, as shown in Eqs. (16)–(19); however, these parameters are not normalized when updating the simplex, so that the simplex can freely deform in the solution space.

We use random values for the initial state of the simplex. The original Nelder–Mead downhill simplex method²⁵ uses the unit vectors lying on each axis of the solution space as initial values. Namely, the initial value of the n th apex \mathbf{a}_n is expressed as follows, except in the case of \mathbf{a}_{2N_e+1} , which is set to be a zero vector:

$$a_{nk} = \begin{cases} 1 & (\text{if } n = k), \\ 0 & (\text{if } n \neq k). \end{cases} \quad (20)$$

However, we cannot set the same initial value as in the original simplex method because the parameters in our situation should satisfy the conditions shown in Eqs. (16) and (18). Therefore, the initial value for $n = 1, \dots, 2N_e$ should be set as follows:

$$\mathbf{a}_n = \frac{\tilde{\mathbf{a}}_n}{\sum_{k=1}^{2N_e} \tilde{a}_{nk}} \quad (21)$$

$$\tilde{a}_{nk} = \begin{cases} 100 & (\text{if } n = k) \\ 1 & (\text{if } n \neq k). \end{cases}$$

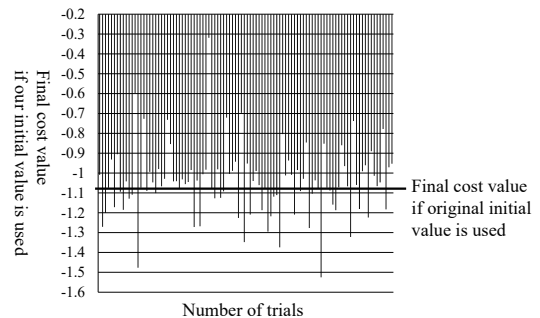


FIG. 7. The final cost value when the random initial values are used.

The $(2N_e + 1)$ th apex is set as follows:

$$a_{2N_e+1,k} = \frac{1}{N_e}. \quad (22)$$

The value of the cost function shown in Eq. (15) was 44.137 for these initial parameters, with certain coefficients set for a_1 , a_2 , a_3 , and a_4 . After optimization using Eq. (14), the cost value was decreased to -1.079 .

Next, we set random values for the initial state of the simplex. We have tried 100 sets of initial values with optimization. The cost value for each set is shown as the vertical bars in Fig. 7. The horizontal line shows the cost value -1.079 . The worst value (the largest value) was -0.319 and the best value (the smallest value) was -1.525 for these 100 experimental results. The average was -1.046 and the standard deviation was 0.173. Out of 100 trials, 36 sets produced better results than when the initial values were set as in Eqs. (21) and (22). Because we can obtain better results if we set the random seed adequately, it is better to use random values for the initial states. On the other hand, compared with the initial cost value 44.137, the range of the final cost value, which varies from -0.319 to -1.525 , is narrow. Therefore, we can state that the optimization method²⁵ stably produces sufficiently good results for a variety of initial values. We therefore did not try to find another way to set the initial values, and we concluded that setting random values for the initial state is sufficient for our purposes.

Here, we explain Eqs. (17) and (19). Mixed-light sources are created by placing certain LED bulbs on a solderless breadboard, with the bulbs being selected based on the mixing ratios calculated in the preceding sections. We represent the number of LED bulbs stuck on a solderless breadboard as N_l . Since the sum of the mixing ratio is 1, we constrain the mixing ratio w_n to be an integer multiple of $1/N_l$. The details of this procedure are given in Algorithm 1.

Fig. 8 shows a specific example of 10 LEDs ($N_l = 10$) selected from 15 different types ($N_e = 15$) stuck on a solderless breadboard.

The cost function (Eq. (15)) becomes a non-smooth discrete function because of the discrete representation of the mixing ratio w_n . The steepest descent method, conjugate gradient method, and Levenberg–Marquardt method are inappropriate for this reason. Instead, the Nelder–Mead downhill simplex

Algorithm 1: Adjustment of the number of bulbs

```

1: for  $n = 1, \dots, N_e$  do  $\alpha_n \leftarrow w_n N_l$ 
2: for  $n = 1, \dots, N_e$  do  $\beta_n \leftarrow \lceil \alpha_n + 0.5 \rceil$ 
3: while  $\sum_{n=1}^{N_e} \beta_n \neq N_l$  do
4:   if  $\sum_{n=1}^{N_e} \beta_n > N_l$  then
5:      $n \leftarrow \text{argmin}(\alpha_n - \beta_n)$ 
6:      $\beta_n \leftarrow \beta_n - 1$ 
7:   end if
8:   if  $\sum_{n=1}^{N_e} \beta_n < N_l$  then
9:      $n \leftarrow \text{argmax}(\alpha_n - \beta_n)$ 
10:     $\beta_n \leftarrow \beta_n + 1$ 
11:   end if
12: end while
13: for  $n = 1, \dots, N_e$  do  $w_n \leftarrow \beta_n / N_l$ 

```

(a)	w_1	w_2	w_3	w_4	w_5	w_6	w_7	w_8	w_9	w_{10}	w_{11}	w_{12}	w_{13}	w_{14}	w_{15}
	0.07	0.10	0.02	0.08	0.10	0.01	0.01	0.04	0.08	0.09	0.01	0.17	0.07	0.09	0.06
(b)	α_1	α_2	α_3	α_4	α_5	α_6	α_7	α_8	α_9	α_{10}	α_{11}	α_{12}	α_{13}	α_{14}	α_{15}
	0.7	1.0	0.2	0.8	1.0	0.1	0.1	0.4	0.8	0.9	0.1	1.7	0.7	0.9	0.6
(c)	β_1	β_2	β_3	β_4	β_5	β_6	β_7	β_8	β_9	β_{10}	β_{11}	β_{12}	β_{13}	β_{14}	β_{15}
	1	1	0	1	1	0	0	0	1	1	0	2	1	1	1
(d)	$\alpha_i - \beta_i$														
	-0.3	0.0	0.2	-0.2	0.0	0.1	0.1	0.4	-0.2	-0.1	0.1	-0.3	-0.3	-0.1	-0.4
(e)	β_1	β_2	β_3	β_4	β_5	β_6	β_7	β_8	β_9	β_{10}	β_{11}	β_{12}	β_{13}	β_{14}	β_{15}
	1	1	0	1	1	0	0	0	1	1	0	2	1	1	0
(f)	w_1	w_2	w_3	w_4	w_5	w_6	w_7	w_8	w_9	w_{10}	w_{11}	w_{12}	w_{13}	w_{14}	w_{15}
	0.1	0.1	0.0	0.1	0.1	0.0	0.0	0.0	0.1	0.1	0.0	0.2	0.1	0.1	0.0

FIG. 8. Example of LED bulb adjustment: (a) Mixing ratio of each LED; (b) (a) times 10; (c) rounded value of (b) (sum 11); (d) value given by subtracting (c) from (b); (e) value obtained by decrementing the value of (c), where (d) is the lowest (sum 10); and (f) (e) times 0.1.

method, simulated annealing method, and genetic algorithm are appropriate. Thus, we use the simulated annealing method based on the Nelder–Mead downhill simplex method.²⁵

A detailed flowchart of the proposed algorithm is shown in Figure 9. Our actual implementation is of the simulated annealing method based on the Nelder–Mead downhill simplex method;²⁵ however, the Nelder–Mead downhill simplex method is too complex to be described in a flowchart. Thus, we only describe the simulated annealing aspect in Fig. 9. Here, T is the temperature, k is the coefficient for decreasing the temperature for each iteration, and r_1 and r_2 are uniform random values used for the simulated annealing method.²⁵ However, we skip the explanation of these parameters to avoid reader confusion because these implementation details may not be of interest to the reader. The measurement of the multispectral data indicated as (a) in Fig. 9 is shown in the Experimental Setup section. The cost function that we use for the evaluation is shown in Eq. (15) (Fig. 9 (d)). If the cost function becomes smaller when we update the mixing ratios \mathbf{w}_1 and \mathbf{w}_2 to $\mathbf{w}_1 + \delta\mathbf{w}_1$ and $\mathbf{w}_2 + \delta\mathbf{w}_2$, then we update these values (Fig. 9 (d)–(e)). The values $\delta\mathbf{w}_1$ and $\delta\mathbf{w}_2$ used for updating the mixing ratios \mathbf{w}_1 and \mathbf{w}_2 are determined via the Nelder–Mead downhill simplex method.²⁵ We skip the explanation of this procedure because it would require several pages

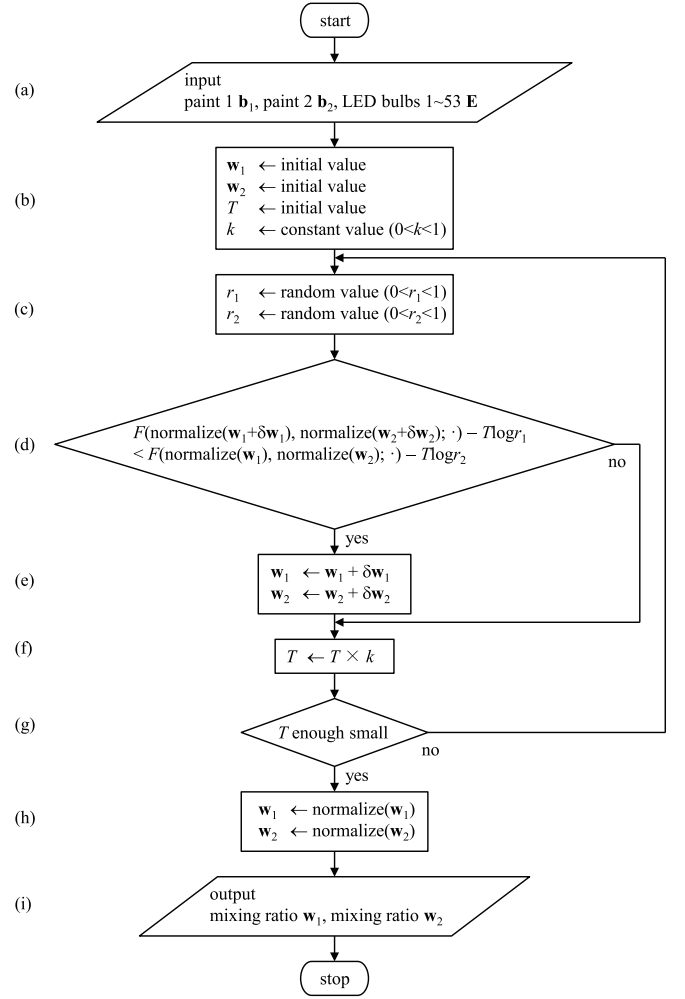


FIG. 9. Detailed algorithm flowchart: (a) database measurement (Experimental Setup section), (b) setting of the initial values (Eq. (21) and (22)), (c) setting of the random values for the simulated annealing,²⁵ (d) the cost function evaluation (Eq. (15)), (e) updating of the mixing ratios with a particular rule,²⁵ (f) cooling down of the temperature used for the simulated annealing,²⁵ (g) checking of the convergence of the simulated annealing,²⁵ (h) normalization of the mixing ratios (Eqs. (16)–(19) and Algorithm 1), (i) end of computation.

because of its complexity. The term “normalize” in Fig. 9 (d) and (h) represents the normalization of the mixing ratios, which is represented as mathematical formulas in Eqs. (16)–(19), and is also represented as a detailed implementation in Algorithm 1.

VI. EXPERIMENT

A. Experimental Setup

Using a hyper-spectral camera HSC-1700, we recorded the optical spectrum data of wavelengths in the range 400–800 nm



FIG. 10. Hyper-spectral camera HSC-1700 manufactured by Eba Japan Co., Ltd.

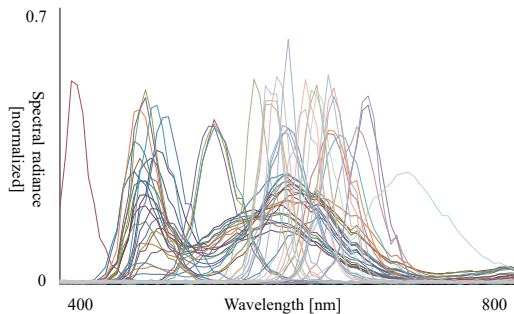


FIG. 11. Database of LED spectral distributions: the normalized spectral distributions are shown in this figure, while the spectral distributions with actual brightness were used in our experiments.

(Fig. 10). This camera can measure the brightness of a total of 81 bands ($N_b = 81$) between 400 nm and 800 nm at intervals of 5 nm. We then measured the spectral distributions of oil paints illuminated by artificial sunlight. The artificial sunlight used was the Probright V, which has a color temperature of 6500 K and Ra98 color-rendering characteristics. After obtaining the spectral distributions of these oil paints, we divided them by the spectral distribution of a diffuse white reflectance standard illuminated by artificial sunlight. The data on the oil paints was obtained by Miyazaki et al.¹⁵

We use LEDs shown in appendix A to achieve metamerism. The diffuse white reflectance standard illuminated by an LED is difficult to measure using the hyper-spectral camera because of the LED's weak radiance; on the other hand, LEDs themselves are too bright to observe directly with a hyper-spectral camera. Therefore, we placed a neutral density (ND) filter in front of the camera to reduce the brightness, and measured 53 types ($N_e = 53$) of LED bulbs. The spectral distributions at the original brightness can be calculated by multiplying the obtained spectral distributions by the reciprocal of the attenuation ratio of the ND filters. We used such original spectral distributions to form the database **E** (Figure 11).

The amount of electrical current that can flow into an LED has an upper limit, so we must maintain constant current within the circuit. For this purpose, we use current regulative diodes (CRDs). Another reason for using CRDs is that the brightness of LEDs should not change regardless of their combination. We designed an electrical circuit by connecting three LEDs in series and connecting the set of three LEDs in parallel. Figure 12 shows the circuit diagram. Figure 13 shows a

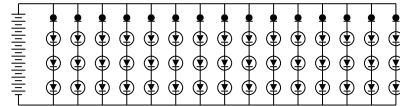


FIG. 12. Circuit diagram of LEDs

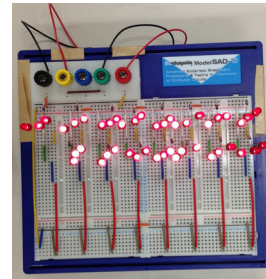


FIG. 13. LEDs stuck on a solderless breadboard

picture of LEDs implemented on a solderless breadboard. The brightnesses of the LEDs are approximately 0.015–30 [cd]; thus, the LEDs are dark compared to halogen lamps, whose brightnesses are approximately 800 [cd]. We therefore implemented 45 LED bulbs ($N_l = 45$) on a solderless breadboard.

The algorithm of the simulated annealing method used for solving Eq. (14) is represented as a nested loop. In the outer loop, the temperature (which is a parameter of the simulated annealing method) was decreased, whereas in the inner loop, the cost function was minimized based on the temperature set in the outer loop. In our experiment, the number of outer loop iterations was set to be 300 and that of the inner loop was set to be 200, making the total number of iterations 60,000 to minimize the cost. The initial temperature was set to be 10, and the coefficient was set to be 0.95, which means that the temperature is multiplied by 0.95 for every outer loop. The computation time of this process was 43 [s] for a database of 53 different types of LEDs, using a single-core Intel Xeon CPU at 2.50 GHz.

B. Experimental Results

We conducted experiments to achieve metamerism using 53 LED colors; two colors (brilliant pink and mars yellow) were used for the oil paints Figure 14 shows the result. Fig. 14(a) shows the canvas painted by brilliant pink and mars yellow. Fig. 14(b) and Fig. 14(c) are the canvas illuminated by mixed source 1 and mixed source 2, respectively. Figures 15 and 16 show the spectral reflectances of the two oil paint colors. The mixing ratios calculated using the proposed method are shown in appendix A. In this experiment, we set the coefficients in Eq. (15) to $a_1 = 100$, $a_2 = 100$, $a_3 = 25$, and $a_4 = 0$. Figure 17 and Figure 18 show the pictures of mixed source 1 and mixed source 2, respectively. Figure 19 and Figure 20 show the pictures of white object illuminated by mixed source 1 and mixed source 2, respectively. Figure 21 and Figure 22 show

the spectral distribution of mixed source 1 and mixed source 2, respectively. Mixed sources 1 and 2 are perceived to be of the same color by the human eye. Figures 23 and 24 show the spectral distributions of brilliant pink and mars yellow when illuminated by mixed source 1; both spectral distributions are unimodal, and their areas and barycenters closely match. Figures 25 and 26 show the spectral distributions of brilliant pink and mars yellow when illuminated by mixed source 2; both spectral distributions have twin peaks, and the brightness of the red peak (which has the longer wavelength) is high for brilliant pink and low for mars yellow. The values of CIE-XYZ, sRGB, and $L^*a^*b^*$ values for this result are shown in Table I. The XYZ values are normalized so that the maximum component becomes 1, and the RGB values are normalized so that the maximum component becomes 255. For each mixed source, an independent maximum value is used, whereas for each set of brilliant pink and mars yellow, the same maximum value is used for both paints, because we do not simultaneously observe each light source but simultaneously observe both paints. The white point for calculating $L^*a^*b^*$ values of the two paints illuminated by mixed source 1 gives the unnormalized XYZ values of mixed source 1, and that of the two paints illuminated by mixed source 2 gives the unnormalized XYZ values of mixed source 2. On the other hand, CIE Standard Illuminant E is used as the white point for calculating $L^*a^*b^*$ values for the two paints in Table I, so that the readers can compare the $L^*a^*b^*$ values in Table I with the spectral reflectance in Figs. 15 and 16, because the spectral reflectance is the same as the spectral distribution of the paints illuminated by the constant spectral distribution of the CIE Standard Illuminant E. The CIE color difference between two paints under mixed source 1 is 22.67, which unfortunately exceeds the just noticeable difference (JND) of 2.3. The human eye can recognize extremely small differences, and therefore the JND value of 2.3 is small. It is difficult to achieve a difference smaller than 2.3, not only for our current research topic but also in most other research cases. However, the color difference under mixed source 2 was 32.09, which is satisfyingly larger than 22.67. These values convince us that our method is successful in computing the intended conditions shown in Fig. 5.

C. Colors Specified by the User

By letting $a_4 > 0$ in Eq. (15), it is possible to design an illumination whose xy-chromaticities are close to a user-specified value \mathbf{u} (Proposed Method section). In this experiment, we used cadmium yellow and cadmium orange oil paints (Figure 27). We conducted the experiment with the user-specified xy-chromaticities $\mathbf{u} = (0.4, 0.5)$ (Figure 28). Figure 29 shows the illumination with coefficients $a_1 = 100$, $a_2 = 100$, $a_3 = 200$, and $a_4 = 0$ in Eq. (15). Figure 30 and Figure 31 are the cadmium yellow and the cadmium orange illuminated by mixed source 1 (Fig. 29(a)) and mixed source 2 (Fig. 29(b)), respectively. Figure 32 shows the illumination with coefficients $a_1 = 100$, $a_2 = 100$, $a_3 = 250$, and $a_4 = 50$. Figure 33 and Figure 34 are the cadmium yellow and the cadmium orange illuminated by mixed source 1 (Figure 29(a)) and mixed

TABLE I. Color values for our results.

	X	Y	Z	R	G	B	L^*	a^*	b^*
Mixed source 1	0.41	1.00	0.06	0	255	0			
Mixed source 2	0.44	1.00	0.07	0	255	0			
Brilliant pink	1.00	0.60	0.45	255	83	123	48.19	50.89	9.89
Mars yellow	0.43	0.32	0.06	173	85	30	36.08	22.87	39.17
Brilliant pink under mixed source 1	0.56	0.32	0.07	120	255	0	31.92	23.73	-4.83
Mars yellow under mixed source 1	0.46	0.88	0.02	92	243	0	29.85	18.17	17.05
Brilliant pink under mixed source 2	0.83	1.00	0.08	255	250	0	34.17	52.14	-2.89
Mars yellow under mixed source 2	0.51	0.78	0.02	171	239	0	30.16	29.51	19.50

source 2 (Figure 29(b)), respectively.

The color of Fig. 32 is closer to the user-specified color shown in Fig. 28 than the color of Fig. 29. The two oil paints (Fig. 27) appear the same (Figure 30) under the illumination in Fig. 29 (a), but they appear differently (Figure 31) under the illumination in Fig. 29 (b), which is the intended result. The two oil paints (Fig. 27) appear to be the same (Figure 33) under the illumination in Fig. 32 (a), but they appear to be different (Figure 34) under the illumination in Fig. 32 (b), which is the intended result.

The color difference shown in Fig. 34 should be large; however, compared to the results shown in Figs. 25 and 26, the color difference is not very large. If the color difference shown in Fig. 34 was large, the actual artwork would be appealing, but the current result is insufficiently appealing because of the smaller color difference than expected. Therefore, we have not performed an actual experiment to confirm the simulated results shown in Figs. 33 and 34. It should be noted, however, that this is a limitation of the physical world, rather than of our proposed method. We examine the limitations of our method in the next section.

D. Analysis of Spectral Distribution

The performance of our method depends on the LED database. If there are 81 orthonormal bases in our spectral distribution database, it becomes possible to express any kind of spectral distribution, and the desired solution can always be obtained (except in an ill-posed situation). LEDs have different light peaks depending on their respective semiconductor materials, and a finite number of semiconductor types have been found (Figure 35). Thus, the spectral distributions that can be obtained by combining LEDs are also finite.

Most of the colors of the LEDs we used fall between red

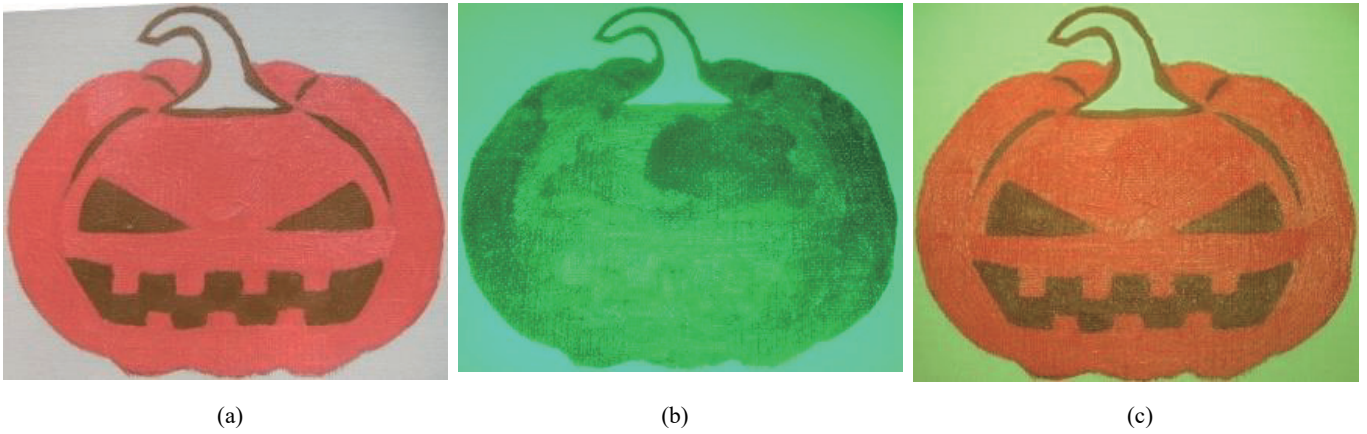


FIG. 14. Experimental result: (a) two types of oil paint, (b) appearance under mixed source 1, and (c) appearance under mixed source 2.

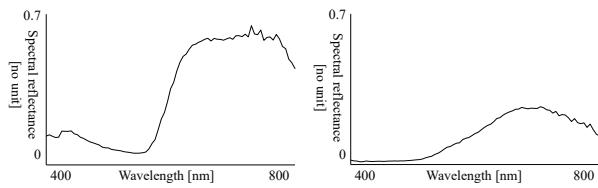


FIG. 15. Spectral reflectance of brilliant pink. FIG. 16. Spectral reflectance of mars yellow.



FIG. 17. The appearance of mixed source 1.



FIG. 18. The appearance of mixed source 2.

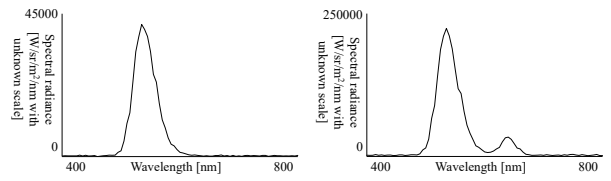


FIG. 21. The spectral distribution of mixed source 1. FIG. 22. The spectral distribution of mixed source 2.

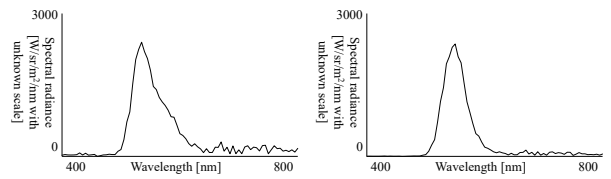


FIG. 23. The spectral distribution of brilliant pink under mixed source 1. FIG. 24. The spectral distribution of mars yellow under mixed source 1.

and yellow (Fig. 11), but there are only a few kinds of LEDs for green and blue in our LED database. The purpose of our research is to evaluate the basic framework of computer-aided art, which designs the illumination under the user-specified database. We have used many easily obtainable LEDs for the



FIG. 19. The RGB color of mixed source 1.



FIG. 20. The RGB color of mixed source 2.

database so that, in general, people can design their desired illumination to create metameric artwork. Because LEDs are commonly obtainable products and are not custom-made, they can produce only a limited number of unique spectral distributions.

By analyzing the spectral distribution database, it is possible to understand how many basis functions are required to describe the distribution.^{15,26-31} Because LEDs are narrow-band sources, they are not suited for principal component analysis; nevertheless, we followed previous works^{15,26-31} and used this method. Although the orthogonal bases computed by principal component analysis do not resemble the spectral distributions of actual LEDs, we can examine the statistical behavior of our database. Because the results of our methods depend

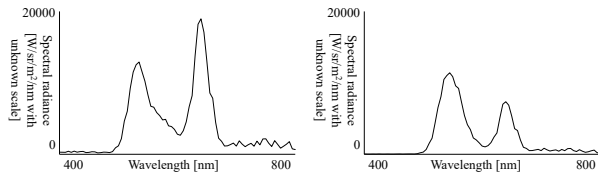


FIG. 25. The spectral distribution of brilliant pink under mixed source 2.

FIG. 26. The spectral distribution of mars yellow under mixed source 2.

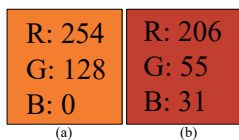


FIG. 27. The RGB colors of cadmium yellow and cadmium orange.

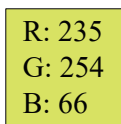


FIG. 28. The RGB colors of xy-chromaticity specified by the user.

strongly on the database, we regard this analysis as important. Principal component analysis is used for simply understanding the rough characteristics of the database, and further detailed analysis is not necessary for our method.

Table II shows the top 20 eigenvalues of the top 20 contributions, and the cumulative contributions obtained by principal component analysis for a database with 53 types of LEDs. Figure 36 shows a graph of the top 20 eigenvalues and Figure

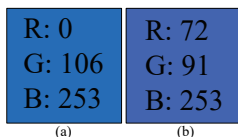


FIG. 29. The RGB color of illumination calculated without user specification: (a) mixed source 1, and (b) mixed source 2.

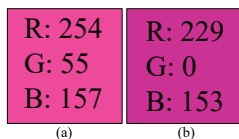


FIG. 30. Mixed source 1 calculated without user specification: (a) cadmium yellow and (b) cadmium orange.

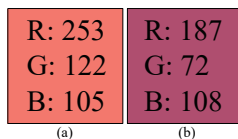


FIG. 31. Mixed source 2 calculated without user specification: (a) cadmium yellow and (b) cadmium orange.

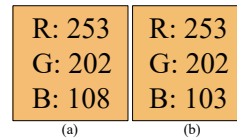


FIG. 32. The RGB colors of illumination calculated with user specification: (a) mixed source 1, and (b) mixed source 2.

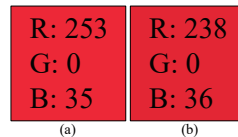


FIG. 33. Mixed source 1 calculated with user specification: (a) cadmium yellow and (b) cadmium orange.

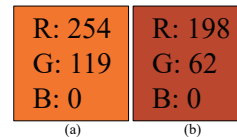


FIG. 34. Mixed source 2 calculated with user specification: (a) cadmium yellow and (b) cadmium orange.

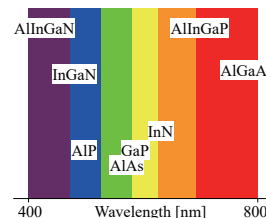


FIG. 35. Colors depending on compounds.

37 shows the top four eigenvectors. As shown in Table II, the cumulative contribution reaches 95% at the 8th eigenvalue, 99% at the 12th eigenvalue, and more than 99.9% at the 20th eigenvalue. From the statistical perspective, if we have 8–12 types of LED with the same spectral distributions as these eigenvectors, the mixture of these 8–12 LEDs can reproduce almost all of the possible varieties of spectral distributions that can be produced using 53 LEDs. However, the shapes of the eigenvectors are different from the actual LEDs, and in addition, negative intensity and negative coefficients cannot occur in the real world; thus, it is difficult to express various spectral distributions using only 8–12 types of LED. Therefore, we have used all 53 LEDs for the database, to allow the design of as many spectral distributions as possible. However, the LEDs we have used do not cover the whole range of the visible-light domain, as is shown in Fig. 11.

Therefore, it is impossible to express an arbitrary spectral distribution using actual LEDs. The simulated annealing method comes close to actualizing metamerism, but the solution is limited by the user-specified constraint, the finite number of existing oil paints, and the finite number of LEDs that have been manufactured. Since the spectral distributions

TABLE II. Cumulative contributions up to the 20th eigenvalue.

Eigenvalue	Contribution (%)	Cumulative distribution (%)	
1	25.03	30.90	30.90
2	16.29	20.11	51.01
3	9.82	12.12	63.13
4	8.07	9.96	73.10
5	6.61	8.16	81.26
6	5.47	6.76	88.02
7	3.06	3.77	91.79
8	2.83	3.49	95.29
9	1.23	1.52	96.81
10	1.11	1.37	98.18
11	0.59	0.73	98.91
12	0.36	0.44	99.35
13	0.18	0.22	99.57
14	0.08	0.10	99.67
15	0.06	0.07	99.74
16	0.05	0.06	99.79
17	0.03	0.04	99.83
18	0.02	0.03	99.86
19	0.02	0.03	99.88
20	0.02	0.02	99.90

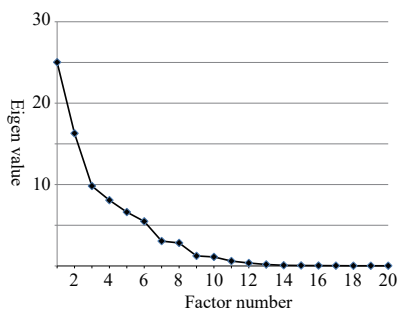


FIG. 36. Eigenvalue plots up to the 20th eigenvalue.

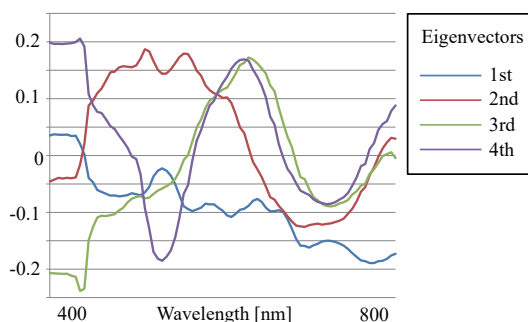


FIG. 37. Graphs of the topmost four eigenvectors.

of our LEDs lack diversity, only a small number of combinations of both light sources and object colors satisfy our aim. To express lights with arbitrary spectral distributions, we also plan to use interference filters or programmable light sources. The use of LEDs that cover the whole range of visible-light wavelengths for our research is also an interesting prospect.

VII. CONCLUSION

We have actualized metamerism with two light sources and two objects. We have designed a method of illumination that will actualize metamerism for given oil paints. We have developed a method to estimate the number of LED bulbs under the given database of spectral distributions. We have performed some experiments and confirmed the efficacy of our method.

Miyazaki et al.¹⁴⁻¹⁶ previously enhanced metamerism by combining paints. On the other hand, the present article describes the enhancement of metamerism by combining LED light sources. By mixing not only the light source but also the paints, we are convinced that metamerism can be enhanced compared with the proposed method and with the existing methods.¹⁴⁻¹⁶

The database of LED spectral distributions obtained in this article is provided online at <http://www.cg.info.hiroshima-cu.ac.jp/~miyazaki/>, so that those who may not have measurement devices for spectral distributions can make metameric artwork using generic LEDs.

ACKNOWLEDGMENTS

This research was supported in part by MEXT KAKENHI Grant No. 15H05925, and in part by JSPS KAKENHI Grant No. 24700176. The authors thank anonymous reviewers for their careful reviews of the article.

Appendix A: THE DETAILS OF OUR LED DATABASE

Tables III and IV show the 53 LEDs from the database used in our method.

After applying our method, we were able to deduce the number of each LED that should be stuck to the solderless breadboard. Table V shows the obtained results from the experiment performed in the Experimental Results section.

¹J. Mitani, "A design method for 3D origami based on rotational sweep," *Comput. Aided Des.* **6**, 69–79 (2009).

²R. D. Hersch and S. Chosson, "Band moiré images," *SIGGRAPH 2004 Papers* 239–247 (2004).

³N. J. Mitra and M. Pauly, "Shadow art," *ACM Trans. Graph.* **28**, 7 (2009) article 156.

⁴Y. Yue, K. Iwasaki, B. Chen, Y. Dobashi, and T. Nishita, "Pixel art with refracted light by rearrangeable sticks," *Comput. Graph. Forum* **31**, 575–582 (2012).

⁵M. Papas, T. Houit, D. Nowrouzezahrai, M. Gross, and W. Jarosz, "The magic lens: refractive steganography," *ACM Trans. Graph.* **31**, 10 (2012) article 186.

TABLE III. Specifications of LEDs.

No.	Model	Manufacturer	Max forward Current (mA)	Forward Voltage (V)
1	AL-5C3UVC-3A-004	A-BRIGHT	20	3.2
2	AL-314IP1C-002	A-BRIGHT	20	3.5
3	GL3HD402E0S	SHARP	20	2.0
4	GL3HY401E0S	SHARP	20	2.0
5	GL5HD44	SHARP	20	2.0
6	GL5JG8	SHARP	20	2.1
7	GL5PR8	SHARP	20	2.1
8	GL5UR2K1	SHARP	20	1.85
9	HCEH-A32A-32	HRD	20	3.3
10	HCEH-A51A-32	HRD	20	3.3
11	HWDH-A51A-12	HRD	20	3.6
12	L-314ED	PARA LIGHT	20	2.1
13	L-314GD	PARA LIGHT	20	2.2
14	L-314YD	PARA LIGHT	20	2.15
15	L-513ET	PARA LIGHT	20	2.1
16	L-513GT	PARA LIGHT	20	2.2
17	L-513LRT	PARA LIGHT	20	1.8
18	L-513YT	PARA LIGHT	20	2.15
19	NSPB300B	NICHIA	20	3.2
20	NSPB500AS	NICHIA	20	3.2
21	NSPB510AS	NICHIA	20	3.2
22	NSPG500S	NICHIA	20	3.5
23	NSPL500DS	NICHIA	20	3.2
24	NSPL510DS	NICHIA	20	3.2
25	NSPL570DS	NICHIA	20	3.2
26	NSPW300DS	NICHIA	20	3.2
27	NSPW500DS	NICHIA	20	3.2

TABLE IV. Specifications of LEDs (cont'd).

No.	Model	Manufacturer	Max forward Current (mA)	Forward Voltage (V)
28	NSPW510DS	NICHIA	20	3.2
29	OS4BFLA131U	OptoSupply	100	3.3
30	OS4WFLA131U	OptoSupply	100	3.3
31	OS5RKDA131U	OptoSupply	150	2.3
32	OS5YADA131U	OptoSupply	150	2.3
33	OS6OGDA131U	OptoSupply	150	2.3
34	OSB5SADSA4D	OptoSupply	20	3.1
35	OSG5DA5111A	OptoSupply	20	3.1
36	OSG5PADSA4D	OptoSupply	20	3.1
37	OSG58DA131U	OptoSupply	150	3.3
38	OSM5DK5JA2D	OptoSupply	20	3.1
39	OSM5DK5111A	OptoSupply	20	3.1
40	OSOR5111A-TU	OptoSupply	20	2.1
41	OSR5PA5201A-VW	OptoSupply	20	2.1
42	OSR5PADSA4D	OptoSupply	20	2.1
43	OSW5DK5JA2D	OptoSupply	20	3.1
44	SDPH53C0C0000	SEIWA	20	3.4
45	SDPW50B0C0000	SEIWA	20	3.8
46	THCW6A-3A25-C	Toricon	20	3.3
47	THWW6A-3A25-C	Toricon	20	3.3
48	TLOH20TP	TOSHIBA	20	2.0
49	TLGE23TP	TOSHIBA	20	2.0
50	TLPYE23TP	TOSHIBA	20	2.0
51	TLSH20TP	TOSHIBA	20	2.0
52	TLYH20TP	TOSHIBA	20	2.0
53	TUCW6D-5A15-A	Toricon	20	3.1

⁶M. Nonoyama, F. Sakaue, and J. Sato, "Multiplex image projection using multi-band projectors," *Proc. IEEE Int'l. Conf. on Computer Vision (ICCV) Workshops* (IEEE, Piscataway, NJ, 2013).

⁷N. Kawai, "Bump mapping onto real objects," *ACM SIGGRAPH 2005 Sketches* (2005) article no. 12.

⁸T. Amano, "Shading illusion: A novel way for 3-D representation on the paper media," *Proc. Procams 2012 Workshop on CVPR2012* (IEEE, Piscataway, NJ, 2012), pp. 1–6, W11.01.

⁹R. Valluzzi, "LEDs illuminat metamerism in abstract art–no 2," <http://www.youtube.com/watch?v=fyJHlinM730>, 2012.

¹⁰R. Bala, K. M. Braun, and R. P. Loce, "Watermark encoding and detection using narrowband illumination," *Proc. IS&T's Seventeenth Color Imaging Conf.* (IS&T, Springfield, VA, 2009), pp. 139–142.

¹¹M. S. Drew and R. Bala, "Sensor transforms to improve metamerism-based watermarking," *Proc. IS&T's 18th Color Imaging Conf.* (IS&T, Springfield, VA, 2010), pp. 22–26.

¹²A. Alsam and G. Finlayson, "Metamer sets without spectral calibration," *J. Opt. Soc. Am. A* **24**, 2505–2512 (2007).

¹³G. D. Finlayson and P. Morovic, "Metamer sets," *J. Opt. Soc. Am. A* **22**, 810–189 (2005).

¹⁴D. Miyazaki, K. Nakamura, M. Baba, R. Furukawa, M. Aoyama, S. Hiura, and N. Asada, "A first introduction to metamerism art," *SIGGRAPH ASIA Posters* (2012).

¹⁵D. Miyazaki, K. Takahashi, M. Baba, H. Aoki, R. Furukawa, M. Aoyama, and S. Hiura, "Mixing paints for generating metamerism art under 2 lights

and 3 object colors," *IEEE Int'l. Conf. on Computer Vision Workshops* (IEEE, Piscataway, NJ, 2013), pp. 874–882.

¹⁶D. Miyazaki, T. Saneshige, M. Baba, R. Furukawa, M. Aoyama, and S. Hiura, "Metamerism-based shading illusion," *The 14th IAPR Conf. on Machine Vision Applications* (IAPR, 2015), pp. 255–258.

¹⁷K. Kobayashi, T. Yamada, A. Hiraishi, S. Nakauchi, "Real-time optical monitoring of microbial growth using optimal combination of light-emitting diodes," *Opt. Eng.* **51**, 123201 (2012).

¹⁸CIE, *Commission internationale de l'Éclairage proceedings, 1931* (Cambridge University Press, Cambridge, UK, 1932).

¹⁹T. Smith and J. Guild, "The C.I.E. colorimetric standards and their use," *Trans. Opt. Soc.* **33**, 73–134 (1931–32).

²⁰G. Laufer, *Introduction to Optics and Lasers in Engineering* (Cambridge University Press, Cambridge, UK, 1996), p. 11.

²¹H. Bradt, *Astronomy Methods: A Physical Approach to Astronomical Observations* (Cambridge University Press, Cambridge, UK, 2004), p. 26.

²²L. Ohannesian and A. Streeter, *Handbook of Pharmaceutical Analysis* (CRC Press, Boca Raton, FL, 2001), p. 187.

²³V. K. Ahluwalia and M. Goyal, *A Textbook of Organic Chemistry* (Narosa Publishing House, New Delhi, 2000), p. 110.

²⁴L. Simonot and M. Hébert, "Between additive and subtractive color mixings: intermediate mixing models," *J. Opt. Soc. Am. A* **31**, 58–66 (2014).

²⁵W. H. Press, S. A. Teukolsky, W. T. Vetterling, and B. P. Flannery, *Numerical Recipes in C: the Art of Scientific Computing* (Cambridge University Press, Cambridge, 1997), p. 994.

²⁶D. B. Judd, D. L. MacAdam, and G. W. Wyszecki, "Spectral distribution of

TABLE V. Mixing ratios (number of LEDs).

No. LED	Light 1	Light 2	No. LED	Light 1	Light 2
1 AL-5C3UVC-3A-004	0	0	28 NSPW510DS	0	0
2 AL-314IP1C-002	0	0	29 OS4BFLA131U	0	0
3 GL3HD402E0S	0	2	30 OS4WFLA131U	0	0
4 GL3HY401E0S	0	0	31 OS5RKDA131U	0	7
5 GL5HD44	0	0	32 OS5YADA131U	0	0
6 GL5JG8	3	1	33 OS6OGDA131U	0	0
7 GL5PR8	0	0	34 OSB5SADSA4D	0	0
8 GL5UR2K1	0	0	35 OSG5DA5111A	0	28
9 HCEH-A32A-32	0	0	36 OSG5PADSA4D	0	1
10 HCEH-A51A-32	0	0	37 OSG58DA131U	41	2
11 HWDH-A51A-12	0	0	38 OSM5DK5JA2D	0	0
12 L-314ED	0	0	39 OSM5DK5111A	0	0
13 L-314GD	0	0	40 OSOR5111A-TU	0	1
14 L-314YD	0	0	41 OSR5PA5201A-VW	0	0
15 L-513ET	0	0	42 OSR5PADSA4D	0	2
16 L-513GT	1	0	43 OSW5DK5JA2D	0	0
17 L-513LRT	0	0	44 SDPH53C0C0000	0	0
18 L-513YT	0	0	45 SDPW50B0C0000	0	0
19 NSPB300B	0	0	46 THCW6A-3A25-C	0	0
20 NSPB500AS	0	0	47 THWW6A-3A25-C	0	0
21 NSPB510AS	0	0	48 TLOH20TP	0	0
22 NSPG500S	0	0	49 TLGE23TP	0	0
23 NSPL500DS	0	0	50 TLPYE23TP	0	1
24 NSPL510DS	0	0	51 TLSH20TP	0	0
25 NSPL570DS	0	0	52 TLYH20TP	0	0
26 NSPW300DS	0	0	53 TUCW6D-5A15-A	0	0
27 NSPW500DS	0	0			

typical daylight as a function of correlated color temperature,” *J. Opt. Soc. Am.* **54**, 1031–1040 (1964).

²⁷J. P. S. Parkkinen, J. Hallikainen, and T. Jaaskelainen, “Characteristic spectra of Munsell colors,” *J. Opt. Soc. Am. A* **6**, 318–322 (1989).

²⁸J. Cohen, “Dependency of the spectral reflectance curves of the Munsell color chips,” *Psychonomical Sci.* **1**, 369–370 (1964).

²⁹L. T. Maloney, “Evaluation of linear models of surface spectral reflectance

with small numbers of parameters,” *J. Opt. Soc. Am. A* **10**, 1673–1683 (1986).

³⁰M. J. Vrhel, R. Gershon, and L. S. Iwan, “Measurement and analysis of object reflectance spectral,” *Color Res. Appl.* **19**, 4–9 (1994).

³¹S. Tominaga and N. Tanaka, “Spectral image acquisition, analysis, and rendering for art paintings,” *J. Electron. Imaging* **17**, 043022 (2008).